Hindawi
Shock and Vibration
Volume 2020, Article ID 8887165, 14 pages
https://doi.org/10.1155/2020/8887165

Research Article

Stress Analysis of Negative Coal Pillar Gob-Side Entry and Its Principle of Preventing Rock Burst

Zhiqiang Wang,[1,2,3,4] Peng Wang ,[1] Lei Shi,[1] Wenyu Lv,[2] Chao Wu,[1] and Jianqiao Luo[1]

[1]*School of Energy and Mining Engineering, China University of Mining and Technology (Beijing), Beijing 100083, China*
[2]*State Key Laboratory of Coal Resources in Western China, Xi'an University of Science and Technology, Xi'an 710054, China*
[3]*Beijing Key Laboratory for Precise Mining of Intergrown Energy and Resources, China University of Mining and Technology (Beijing), Beijing 100083, China*
[4]*National Demonstration Center for Experimental Safe Coal Mining and Geological Guarantee Education, China University of Mining and Technology (Beijing), Beijing 100083, China*

Correspondence should be addressed to Peng Wang; bqt1800101026@student.cumtb.edu.cn

Received 3 July 2020; Revised 28 September 2020; Accepted 7 October 2020; Published 12 November 2020

Academic Editor: Xuesheng Liu

Gob-side entry is an area where it is difficult to prevent and control the frequent occurrence of rock burst. Based on "Longwall Mining with Split-level Gateways" (LMSG), this paper puts forward the technology of preventing rock burst by a new gob-side entry (NCPG). The abutment pressure distribution of LMSG shows that the stress peak of solid coal is lower than the conventional panel, and the width of the limit equilibrium zone is also reduced by a small percentage. After the narrow coal pillar gob-side entry has been excavated, the peak stress in solid coal increases, and the width of the limit equilibrium zone decreases, so the practical stress concentration increases. However, the NCPG located in areas of lower stress. The peak stress in solid coal of the NCPG does not increase, but the width of the limit equilibrium zone increases, so the practical stress concentration decreases. NCPC makes the concentrated stress transfer into the deep coal body and plays the role of pressure avoidance. Compared with the narrow coal pillar gob-side entry, the NCPG reduces the energy stored in coal and rock masses and increases the energy consumption. It has significantly improved the regionality, initiative, safety, and timeliness of rock burst prevention in deep high-stress coal seam mining.

1. Introduction

With the large-scale exploitation of coal resources in China, the shallow and central coal resources are less and less. Many mining areas have entered the deep mining state one after another. Rock burst has become one of the most dangerous dynamic disasters [1–3]. According to statistics, rock burst mines are distributed over nearly 100 mining areas in 19 provinces of China. Currently, the majority of the documented rock burst events have occurred in a local area of gate roads within a limited range around the coal face [4, 5]. Statistics show that there are 675 rock burst events in various mining areas such as Huating, Yima, Hegang, and Shandong, and it is found that 91% of rock burst accidents occur in the roadway, especially the roadway along the goaf [6, 7]. Therefore, it is of great theoretical and practical significance to study the rock burst mechanism and prevention methods of the roadway along the goaf.

Many scholars have studied the mechanism of rock burst [8–10]. Although there is no agreed upon definition of rock burst among researchers, it is generally accepted that rock burst is the sudden release of elastic strain energy in rock masses under high local stresses, resulting in rock fragmentation, ejection, projection, and even earthquakes [11]. Existing research mainly concentrates on the monitoring, prediction, and prevention of rock burst [12, 13]. The theory and practice show that the prevention and control of rock

burst are essentially to control the stress state of coal rock mass or reduce the generation of high stress of coal rock mass [14]. At present, China's rock burst prevention and control technology can be summarized into two aspects. One is to weaken the coal body to reduce impact properties [15], which includes water injection in coal seam and presplitting blasting. The second is to transfer stress or release strain energy, which generally includes blasting destressing [16], borehole destressing [17], hydraulic fracturing [18], sleeve fracturing [19], etc. These technical measures have achieved certain results, but there are still certain deficiencies, mainly reflected in locality, passiveness, danger, poor timeliness, and contradictions with production.

Longwall mining is a highly productive underground mining system. It originated in Britain in the early 18th century and began to be used in China in the 1930s. Coal mining activities will inevitably lead to the redistribution of the original rock stress. There is a certain range of low-stress areas in the solid coal side of the goaf. Arrangement of the roadway in this low-stress area can avoid stress concentration and facilitate the maintenance of the roadway; at the same time, by reducing the width of the coal pillar, coal resource waste can be reduced. Therefore, the gob-side entry driving technology with a 3–6 m narrow coal pillar is widely used [20, 21]. However, is it still applicable when the mine is under high pressure with the risk of rock burst? The practice of narrow pillar gob-side entry in Huafeng coal mine and Yuejin coal mine in deep mining showed that there were still many times where rock burst occurred in the gob-side entry, which were not ideal for the prevention of rock burst [17, 22]. This was because the distribution law of the abutment pressure is not clear after the entry excavation along the goaf. What kind of roadway arrangement is beneficial to the prevention of rock burst is a problem worthy of consideration.

The novel approach "Longwall Mining with Split-level Gateways (LMSG)," which is an innovative patent invented by Dr. J.L. Zhao in 1998 at China University of Mining and Technology (Beijing) [23], is being employed for the coal mine of interest [24]. Based on the LMSG, this paper proposes the layout of "Negative Coal Pillar Gob-side Entry (NCPG)." By analyzing the stress distribution of the surrounding rock of the gob-side entry with narrow and negative coal pillar, the respective rock burst risk is discussed. Finally, the Huafeng coal mine has adopted three layout methods of wide coal pillar, small coal pillar, and negative coal pillar for practical verification.

2. Abutment Pressure of LMSG

Roadways of the conventional longwall top coal caving (CLTCC) are generally arranged along the coal seam floor and located at the same level, as shown in Figure 1(a). The LMSG is a method suitable for mining thick coal seams. The difference between it and CLTCC is that the two roadways of the panel are arranged along different levels, one of which is arranged along the floor of the coal seam, and the other is arranged along the roof of the coal seam. There is a trapezoidal coal body left unmined along the edge of the mined-out area, as shown in Figure 1(b). The trapezoidal coal body is lifted by each hydraulic support up to 3°, and the final lifting angle is 15°.

2.1. Limit Equilibrium Zone Width. After mining out of the panel in CLTCC, the expression of the solid coal limit equilibrium zone width is [25]

$$x_0 = \frac{m}{2\xi f} \ln \frac{K\gamma H + C\cot\varphi}{\xi[p_1 + C\cot\varphi]}, \quad (1)$$

where K is stress concentration factor; m is coal seam mining thickness; H is cover depth; p_1 is the lateral support stress acting on the coal wall; C is cohesion; φ is internal friction angle; f is friction factor of coal seam and roof; ξ is triaxial stress coefficient: $\xi = (1 + \sin\varphi)/(1 - \sin\varphi)$.

From equation (1), it is found that the limit equilibrium zone width is directly proportional to the mining thickness of the coal seam and inversely proportional to the lateral support stress.

In the mining of the panel in CLTCC, the mining height along the dip is unchanged, and the support body of the coal wall fails after mining. However, the mining height of the trapezoidal coal body section in the LMSG gradually decreases, and the trapezoidal coal body can still play a similar role as a support body to provide certain support stress for the solid coal with good integrity. Therefore, it can be predicted that the width of the limit equilibrium zone in the LMSG will change to some extent. Establish the limit equilibrium mechanical model and study distribution characteristics of the limit equilibrium zone, as shown in Figure 2. In the figure, m is coal seam mining thickness; $m/2$ is the height of trapezoid coal body; θ is dip angle of trapezoidal coal body; l is the length of trilateral coal body; a is the upper length of trapezoidal coal body; Σh is immediate roof thickness; γ_1 is immediate roof bulk density; α is rock break angle; γ_2 is coal bulk density; σ_x is horizontal stress, σ_y is vertical stress.

The mechanical model needs to meet the following two basic assumptions:

(1) There is a slip plane with relative motion between the coal and the rock layer at the roof and floor. The shear stress on the slip plane is $C + f\sigma_x$

(2) The position of vertical stress peak is at the boundary between the stress limit equilibrium region and the elasticity

After mining the panel, the immediate roof collapse gangue acts on the trapezoidal coal body. Then the weight of gangue and trapezoidal coal pillar is G, approximately:

$$G = \sum h\left(l + 2a - \cot\alpha \sum h\right)\gamma_1 + \frac{l + 2a}{4} m\gamma_2. \quad (2)$$

Trapezoidal coal body provides some support stress for solid coal. It is mainly the friction force between the coal body and the bottom stratum. The lateral protection force p_2 obtained by Newtonian mechanics is

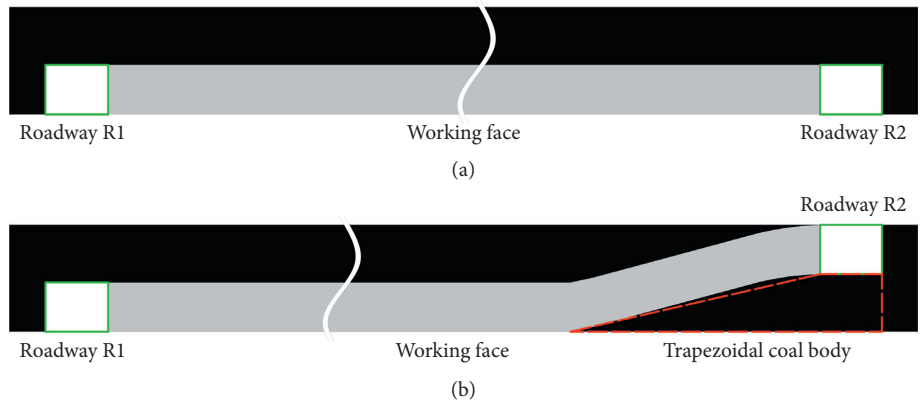

Figure 1: Active panel diagram. (a) CLTCC. (b) LMSG.

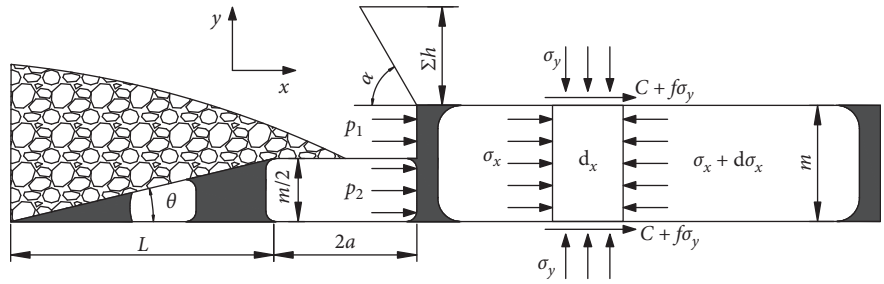

Figure 2: Limit equilibrium mechanical model in the LMSG.

$$p_2 = \frac{f \cdot G}{m/2} = \frac{2f}{m}\left[\sum h\left(l + 2a - \cot\alpha \sum h\right)\gamma_1 + \frac{l + 2a}{4} m\gamma_2\right]. \tag{3}$$

According to the limit equilibrium theory, establish the stress equilibrium equation of lateral coal body:

$$2\left(C + f\sigma_y\right)\mathrm{d}x + m\sigma_x + p_2 - m\left(\sigma_x + \mathrm{d}\sigma_x\right) = 0, \tag{4}$$

$$2C + 2f\sigma_y - m\frac{\mathrm{d}\sigma_x}{\mathrm{d}x} = 0. \tag{5}$$

Known limit equilibrium conditions are

$$\sigma_y = \frac{1 + \sin\varphi}{1 - \sin\varphi}\sigma_x + \frac{2C\cos\varphi}{1 - \sin\varphi}. \tag{6}$$

Differentiate the two sides of equation (6) to get

$$\frac{\mathrm{d}\sigma_y}{\mathrm{d}x} = \frac{1 + \sin\varphi}{1 - \sin\varphi}\frac{\mathrm{d}\sigma_x}{\mathrm{d}x} = \xi\frac{\mathrm{d}\sigma_x}{\mathrm{d}x}. \tag{7}$$

Simultaneous equations (5) and (7) are available:

$$2C + 2f\sigma_y - m\frac{1}{\xi}\frac{\mathrm{d}\sigma_x}{\mathrm{d}x} = 0. \tag{8}$$

Solve this differential equation and get

$$\sigma_y = C_0 e^{(2f\xi/m)x} - \frac{C}{f}. \tag{9}$$

At the edge of goaf, when $x = 0$, the lateral support stress is $\sigma_x = p_1 + p_2$. Substitute σ_x into equation (5) and perform the triangle identity transformation:

$$\sigma_y = \xi\left(p_1 + p_2 + C\cot\varphi\right) - C\cot\varphi. \tag{10}$$

Substituting equation (9) into equation (10) yields

$$C_0 = \xi\left(p_1 + p_2 + C\cot\varphi\right) - C\cot\varphi + \frac{C}{f}. \tag{11}$$

After the mining of the panel is completed, the support effect of the roadway support on the solid coal side has failed, so $p_1 = 0$, and $f \approx \tan\varphi$, so equation (11) is simplified:

$$C_0 = \xi\left(p_2 + C\cot\varphi\right). \tag{12}$$

Combined with equations (3), (9), and (12), the following equation can be obtained:

$$\sigma_y = \left[\xi\left[\frac{2f}{m}\sum h\left(l + 2a - \cot\alpha\sum h\right)\gamma_1 + f\frac{l + 2a}{4}m\gamma_2 + C\cot\varphi\right]\right]e^{(2f\xi/mx)} - C\cot\varphi. \tag{13}$$

Assuming that the peak value of stress is $\sigma_{y\max} = K_L \gamma H$, K_L is the stress concentration factor; substituting into equation (13), the width of the mining limit equilibrium zone in the LMSG can be obtained:

$$x_L = \frac{m}{2\xi f} \ln \frac{K_L \gamma H + C \cot \varphi}{\xi [(2f/m) \sum h (l + 2a - \cot \alpha \sum h) \gamma_1 + f ((l + 2a)/4) m \gamma_2 + C \cot \varphi]}. \quad (14)$$

Then specific parameters of the panel were used to comparatively analyze the width of the limit equilibrium zone in CLTCC and LMSG, where H is 500 m; m is 6 m; φ is 20°; C is 1.0 MPa; γ is 27 kN/m^3; Σh is 5 m; γ_1 is 20 kN/m^3; α is 75°; γ_2 is 14 kN/m^3; K is 4; K_L is 4; l is 11.2 m; a is 4 m. Substituting into equations (1) and (14), respectively, the width of the limit equilibrium zone of the CLTCC is $x_0 = 7.42$ m. The width of the limit equilibrium zone of the LMSG is $x_L = 6.92$ m, which is reduced by 0.5 m. The reduction ratio of the limit equilibrium zone width is 0.32/7.42 = 6.7%.

The above theoretical analysis shows that, compared with CLTCC, the peak position of the abutment pressure of LMSG is shifted to the goaf side, and the range of limit equilibrium zone is reduced, but the reduced distance is very small compared with the entire limit equilibrium zone.

2.2. Peak Stress. The width of the limit equilibrium zone is one of the characteristics of the abutment pressure, and the peak stress is another. Physical modeling is an effective way to study rock strata behavior and has been extensively used in China [26]. In this paper, it is used to study the peak stress of the abutment pressure of the LMSG. Large-scale 2D physical models were built in China University of Mining and Technology (Beijing) for Zhen Chengdi coal mine. According to the field data of the 22204 panel [27], the developed engineering properties are given in Table 1 and were used to develop equivalent model materials properties.

The author had carried out a physical modeling of another panel of Zhen Chengdi coal mine in the early stage, which was similar to the geological conditions of the object in this paper, so the same similarity ratio data was cited [27]. Equivalent model materials used consisted of aggregate (fine sand) and cement materials (lime and plaster). The geometric scaling factor of $\alpha_L = 100:1$, the density factor of $\alpha_\gamma = 1.5:1$, and the time factor of $\alpha_t = 10$ were used for physical modeling studies. Equivalent material parameters and the proportion of different constituents in the physical model are given in Table 2. Type-CM-2B static strain gauges were embedded into model materials to measure strains at strategic locations that were built during the construction stage and then converted to stress values.

The dimensions of the physical models were 1800 mm (length) × 160 mm (width) × 1300 mm (height). According to the height and proportion of the model, the top of the test bench is pressurized by 5 kg. Plane-stress simulations were used. The physical modeling initial model and results are shown in Figure 3.

22204 panel is mined by CLTCC from 0 m to 135 m. From Figure 3(b), we can see that the damage height of the overlying strata is about 80 m, and the damage state is symmetrical along the centerline of the panel. After 135 m, it is mined by LMSG. The height of the trapezoidal coal body is half of the coal seam thickness. The damage height of the overlying strata in this range is about 70 m, which is reduced by 10 m. From Figure 3(c), we can see that one end of the basic roof key block A is supported by solid coal wall rock, and another end is hinged with the key block B to form the voussoir structure. There is a certain height of free space between the key block A and the trapezoidal coal body. The trapezoidal coal body is located in the voussoir beam shelter area, which only bears the weight of the collapsed gangue without the force of the key block A.

From Figure 3(d), we can see that, in CLTCC, the floor stress is symmetrically distributed, the maximum stress of the solid coal floor on both sides is about 25 MPa, the floor stress of the goaf is released to about 2.0 MPa, and the rock stress at the edge of the goaf is 0.6 MPa. Meanwhile, in LMSG, the floor stress of the solid coal side is about 22 MPa, which is 3 MPa less than that of the CLTCC. The reason is that the damage height of the overlying strata is reduced, which makes the load transmitted to the solid coal side reduced. The stress of the trapezoidal coal floor is 0.3 MPa, which is in the low-stress area. Thus, the trapezoidal coal body is under the cover of the voussoir beam structure and only bears the weight of the immediate roof.

As regards comprehensive theoretical analysis and physical model research results, compared with CTLCC, the peak value of the abutment pressure solid coal side in LSMG is reduced, and the peak position shifts slightly to the goaf. Therefore, the LSMG elastoplastic partition and abutment pressure distribution are shown in Figure 4. The stress on the solid coal can be divided into five zones: I, destressed yield zone; II, overstressed plastic zone; III, overstressed elastic zone; IV, premining vertical stress zone; and V, pressure-free zone. The vertical stress of the pressure-free zone is less than the premining vertical stress.

3. Stress Distribution of Gob-Side Entry

3.1. Stress Distribution of Narrow Coal Pillar Gob-Side Entry. After panel mining, O-X breakage occurred in the basic roof along the dip and in turn experienced the processes of breakage, rotary sinking, caving, and stability. Within a certain range, the coal body yielded and the stress within the coal body was redistributed. Yield failure occurred in the coal body within a certain range as well as redistribution of stress in the coal body.

According to destruction characteristics and the stress state of the coal body, the bog-side entry with narrow coal

Table 1: Thickness and physical or mechanical properties of rock strata.

Rock strata	Thickness (m)	Density (kg·m^{-3})	Compressive strength (MPa)
Medium sandstone	50	2500	27.2
Mudstone	8	2500	9.4
Siltstone	13	2600	27.0
Limestone	6	2500	31.4
Shale	7	2550	9.40
Sandy mudstone	6	2500	20.6
Siltstone	10	2600	31.4
Mudstone	5	2500	9.70
Coal	6	1400	4.49
Mudstone	3	2500	9.70

Table 2: Material parameters and proportion of different constituents in physical model materials.

Rock strata	Density (kg·m^{-3})	Proportion number	Materials	Aggregate: materials	Lime: plaster (lime: soil)
Medium sandstone	1.67	6 : 5 : 5	Sand : cement : plaster	6 : 1	5 : 5
Mudstone	1.66	8 : 6 : 4	Sand : lime : plaster	8 : 1	6 : 4
Siltstone	1.70	6 : 5 : 5	Fine sand : lime : plaster	6 : 1	5 : 5
Limestone	1.68	10 : 9 : 1	Fine sand : lime : plaster	10 : 1	9 : 1
Shale	1.69	10 : 6 : 1	Fine sand : lime : plaster	8 : 1	9 : 1
Sandy mudstone	1.60	8 : 6 : 4	Fine sand : lime : plaster	10 : 1	8 : 2
Siltstone	1.70	6 : 5 : 5	Fine sand : lime : plaster	6 : 1	5 : 5
Mudstone	1.66	8 : 6 : 4	Sand : lime : plaster	8 : 1	6 : 4
Coal	1.02	10 : 1 : 0	Fine sand : lime : soil	10 : 1	
Mudstone	1.66	8 : 6 : 4	Sand : lime : plaster	8 : 1	6 : 4

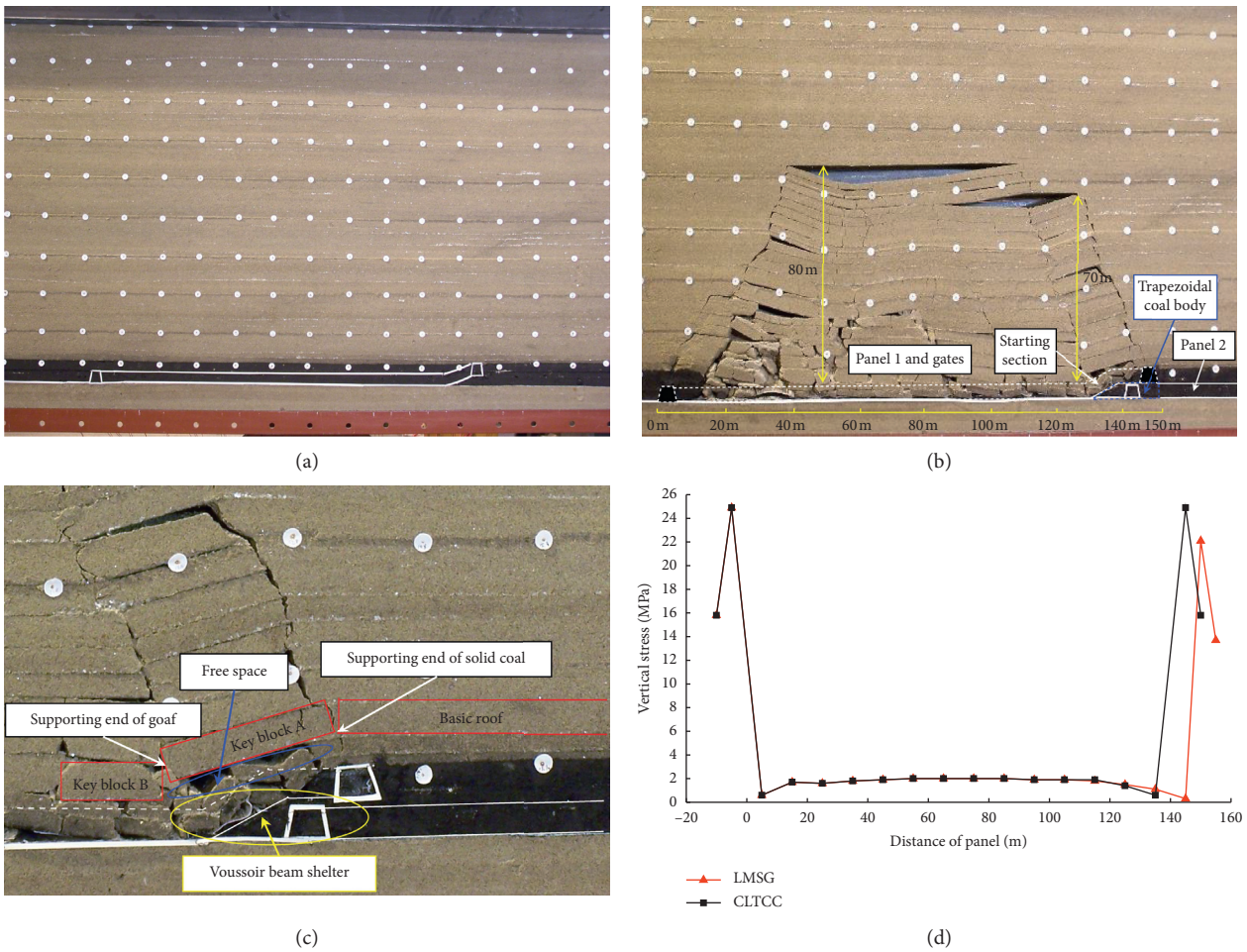

Figure 3: Physical modeling initial model and results. (a) Initial model. (b) Overlying strata characteristics. (c) Partial enlarged view. (d) Floor vertical stress.

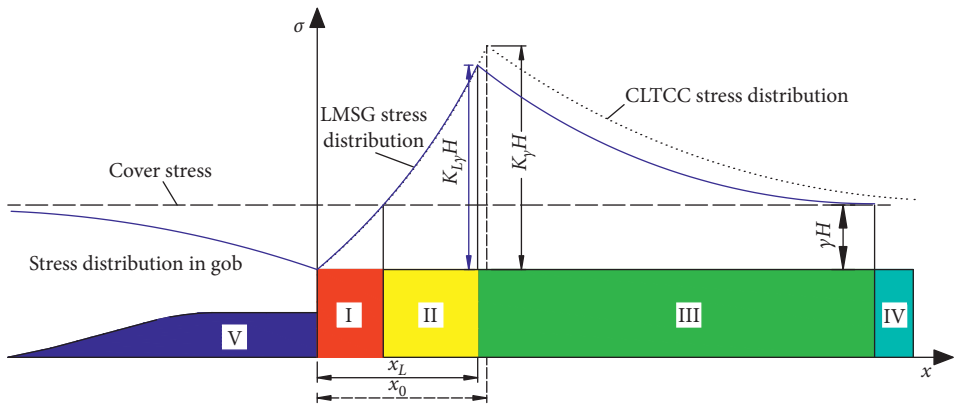

Figure 4: Elastoplastic zone and abutment pressure of LMSG.

pillar is driven into the plastic zone next to the yield zone after the overburden movement of the upper face is stable. The distribution of the abutment pressure of solid coal before gob-side entry excavation is shown in blue solid curve 1 in Figure 5, and the width of the limit equilibrium zone is x_0. In previous theories, the distribution of abutment pressure after the narrow coal pillar gob-side entry driving is not clear, and it is believed that, after the gob-side entry excavation, the peak position of abutment pressure is shifted toward the solid coal by the distance which is the sum of the coal pillar and the roadway width [25]. We can think about this problem by assuming an increase in the length of the panel. If the length of the panel is increased by $l + a$, the peak position of abutment pressure is shifted by $l + a$ towards the inside of the coal body, when the width of the limit equilibrium zone is x_0', and $x_0' = x_0$. At this time, the distribution of abutment pressure should be as shown in the blue-dotted curve in Figure 5. In fact, the coal pillar has undergone plastic failure under the influence of mining in the mined-out panel, and the internal cracks are highly developed. When affected by the excavation of the gob-side entry again, even if the cracks inside the coal pillar develop further, its bearing capacity drops again, but it does not lose its bearing capacity and can still bear a small load. Therefore, after excavation of the gob-side entry, the loading in the coal pillar decreases, while the peak value of the solid coal abutment pressure increases. The moving distance of the peak position of the abutment pressure should be less than $l + a$ and greater than $(l + a)/2$. Then, the distribution of the abutment pressure of solid coal after gob-side entry excavation should be shown in the red solid curve in Figure 5. Therefore, the actual peak value increases, while the width of the limit equilibrium zone decreases, and the degree of stress concentration in the solid coal increases.

3.2. Stress Distribution of NCPG. Negative coal pillar gob-side entry (NCPG) is based on LMSG, which arranges the gob-side entry of the successive panel in the trapezoidal coal body. The actual meaning of the coal pillar is the distance between the roadway and the edge of the goaf. To scientifically express the layout of NCPG, a plane rectangular coordinate system is established by taking the intersection of the edge of the goaf and the coal floor as the origin of coordinates. Take the distance between the left side of the gob-side entry and the mined-out area as the coal pillar width, as shown in Figure 6. There are three types of roadway layout; namely, roadway 1 ($x_1 > 0$) is a positive coal pillar, roadway 2 ($x_2 = 0$) is a zero coal pillar, and roadway 3 ($x_3 < 0$) is a negative coal pillar. Normally, NCPG is offset to goaf by twice the width of the roadway.

The solid coal abutment pressure distribution of LMSG is shown in the blue curve in Figure 7. The NCPG is excavated in trapezoidal coal pillars, and the load it bears is transferred to the goaf and solid coal. Because the trapezoidal coal body has been relieved of pressure and only bears the weight of the collapsed gangue, the load transferred to the surrounding rock is small. We can think that the stress in the goaf is unchanged. Because the distance between the roadway and the solid coal is large, the influence on the abutment pressure distribution of the solid coal side is lower, as shown in the red curve in Figure 7. The limit equilibrium zone moves closer to a very small distance, and the peak stress increases slightly. The actual distance between the roadway and the peak of the abutment pressure increases and the increased width is the distance that the roadway moves closer to the goaf, which is usually the width of the roadway; the width of the limit equilibrium zone is recorded as x_L. Adopting the conventional technology of staying along the roadway, the distance between the roadway and the peak abutment pressure is less than 7.42 m. Meanwhile, with the negative coal pillar roadway layout, this distance is greater than $6.92\,m + 4\,m = 10.92$ m, which increases by 53.9%. At the same time, the NCPG has another characteristic compared with CLTCC. The stress in the coal walls on both sides of the NCPG is less than the cover stress. Figure 7 shows that the range where the abutment pressure is lower than the cover stress is the sum of zone I and the range from the gob-side entry to the edge of goaf. The gob-side entry arrangement in the goaf is always unaffected by the front and side abutment pressure.

Therefore, the NCPG is far away from the overstressed plastic zone, which can better avoid the influence of high-stress concentration and realize the effect of transferring the peak stress to the deep coal body. The stress concentration of NCPG is lower than that of the conventional gob-side entry.

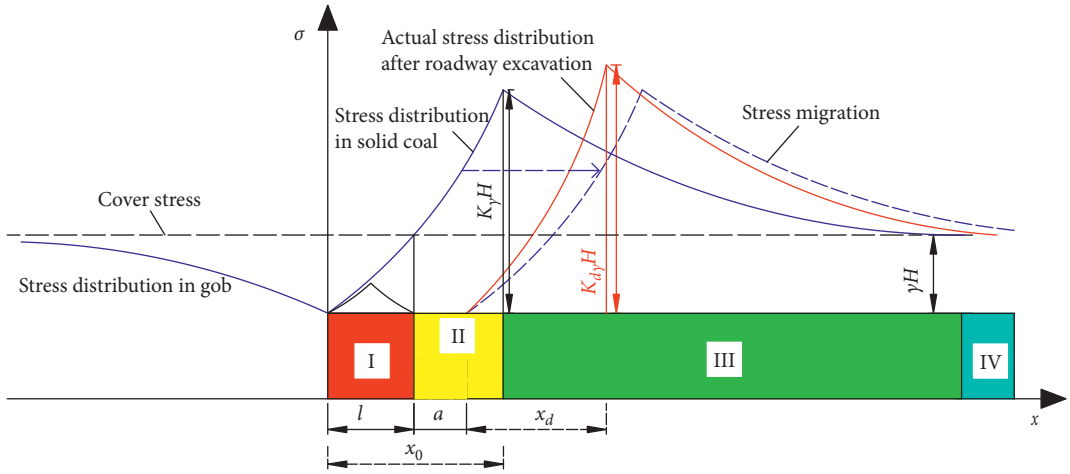

Figure 5: Distribution of abutment pressure of narrow coal pillar gob-side entry.

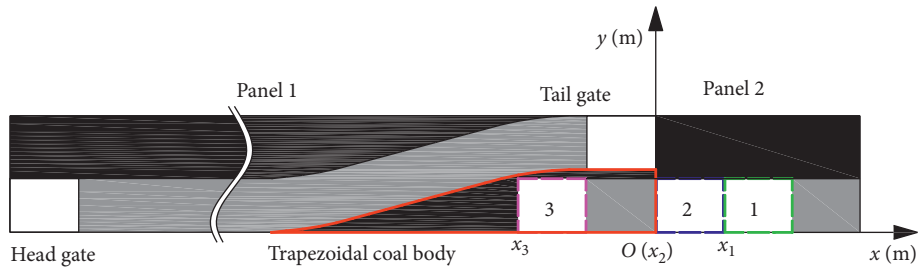

Figure 6: Roadway layout of LMSG.

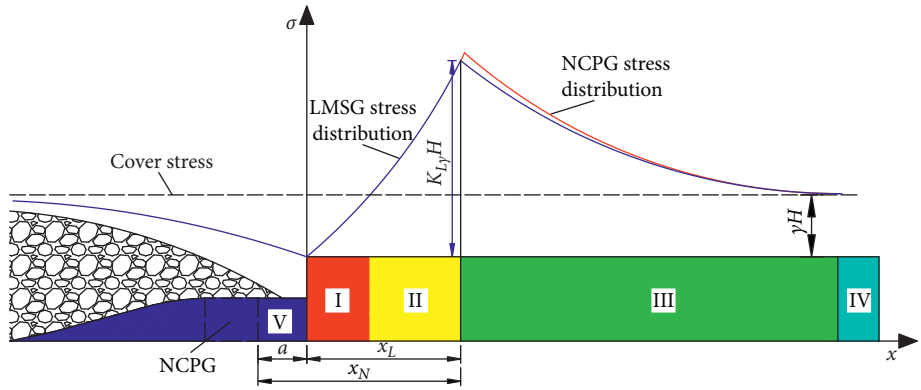

Figure 7: Abutment pressure of NCPG.

4. Analysis of Gob-Side Entry Using Numerical Modeling

The FLAC^{3D} numerical simulation experiment method is used to establish numerical models for the conventional gob-side entry and NCPG, respectively, and verify the aforementioned theoretical analysis results. The dimensions of the two models are 280 m (length) × 20 m (width) × 120 m (height). Mohr-Coulomb criterion is adopted. Table 3 lists the rock mass engineering properties by referring to the previous research data in the previous studies [28].

The coal seam is 500 m deep, and the thickness of rock strata above the coal seam is 105 m. The uncovered overlying rock load above was calculated to be 389 m × 0.025 KN/m^3 = 9.7 MPa, and it was loaded vertically down on top of the model. The side boundaries were roller-constrained and the bottom boundary was fixed both horizontally and vertically.

The simulation schemes are as follows: (1) After the excavation of the panel in CLTCC is completed, 5 m, 6 m,

Table 3: Mechanical parameters for rock masses.

Lithology	Thickness (m)	Density ($kg \cdot m^{-3}$)	Bulk modulus (GPa)	Shear modulus (GPa)	Cohesion (MPa)	Tensile strength (MPa)	Friction angle (deg.)
Medium sandstone	50	2500	5.90	4.23	8.82	2.75	28
Mudstone	8	2500	3.2	3.85	8.7	1.50	25
Siltstone	13	2600	4.88	3.45	26.6	2.85	35
Limestone	6	2500	3.88	3.45	9.24	1.38	30
Shale	7	2550	3.85	1.84	8.7	1.5	29
Sandy mudstone	6	2500	3.2	3.5	10.2	1.05	30
Siltstone	10	2600	6.23	4.95	18.8	2.75	32
Mudstone	5	2500	3.2	3.85	8.7	1.50	25
Coal	6	1400	1.2	1.1	1.0	0.45	20
Mudstone	3	2500	3.2	3.85	8.7	1.50	25
Limestone	6	2500	3.88	3.45	9.24	1.38	30
Siltstone	3	2600	4.88	3.45	26.6	2.85	35
Medium sandstone	7	2500	5.90	4.23	8.82	2.75	28
Limestone	20	2500	6.23	5.9	10.8	2.75	32

and 7 m coal pillars are left to excavate gob-side entry. (2) After the excavation of the panel in LMSG is completed, the NCPG (−8 m) excavation is simulated. The vertical stress simulation results after gob-side entry excavation are shown in Figure 8. Extract the vertical stress of solid coal, as shown in Figure 9.

Figure 9 shows that the peak value of vertical stress in LMSG is lower than that of CLTCC. The vertical stress in the trapezoid coal body is lower than the premining vertical stress. The peak position of the vertical stress in LMSG is 5 m from the goaf, when that in CLTCC is 6 m from the goaf. Compared with CLTCC, the vertical stress peak of LMSG is closer to the goaf, but the offset distance is small relative to the width of the limit equilibrium zone, which is consistent with physical modeling results.

Figures 8(a)–8(c) show the vertical stress distribution in the solid coal after the narrow coal pillar gob-side entry is excavated. We can find that the roadway is in the low-stress area. After the roadway is excavated, the peak stress shifts to deep of the solid coal. The specific data in Figure 9 shows that, after the roadway is excavated, the width of the limit equilibrium zone of the three is reduced from 6 m to 4 m. The moving path of stress peak is not an equidistant offset of the sum of coal pillar width and roadway width. After the roadway is excavated, the internal stress of the solid coal increases significantly, and the internal stress of the coal pillar decreases accordingly. With the increase of coal pillar width, the solid coal stress decreases, and the coal pillar stress increases. The peak stress of solid coal increases and the range of limit equilibrium area decreases, which can prove that its stress concentration increases. The numerical simulation results are consistent with the theoretical analysis results.

Figure 8(d) shows the vertical stress distribution of the NCPG after excavation. The gob-side entry is located in the low-stress area, which is mostly tensile stress. Figure 9 shows that, after NCPG excavation, the coal body stress under the goaf increases slightly, but it is still lower than the rock stress, while the solid coal stress does not change. The peak stress of solid coal is lower than that of the narrow coal pillar gob-side entry. The distance between the right side of NCPG and the peak position of vertical stress is 5 m + 4 m = 9 m. Compared with the narrow coal pillar gob-side entry, it is equivalent to an increase in the width of the limit equilibrium zone by 5 m, and the increase ratio exceeds 50%. By changing the location of the roadway, the solid coal stress of NCPG does not change, while the limit equilibrium zone width increases significantly, so the stress concentration is significantly reduced.

5. Mechanism to Prevent Rock Burst

According to the structural characteristics and stress distribution of surrounding rock of negative coal pillar gob-side entry, the principle of preventing rock burst can be obtained, as shown in Figure 10.

The NCPG layout prevention mechanism of rock burst is mainly reflected in the following three aspects:

(1) The peak stress of lateral support pressure is reduced, the degree of high-stress concentration is reduced, and the stress peak is transferred to the deep part of the coal body

(2) The width of the yielding coal body increases, the elastic energy accumulated in the coal seam is released, and the impact energy dissipation of the solid coal side is increased

(3) The free space blocks the energy transmission path, and the large deformation characteristics of the gangue cushion the impact of dynamic load

The essence of preventing rock burst is to reduce the high stress in coal and rock. It can be seen from the foregoing analysis that high stress is mainly concentrated on the solid coal side of the roadway, so the risk of rock burst on the solid coal side is much greater than that on the goaf side.

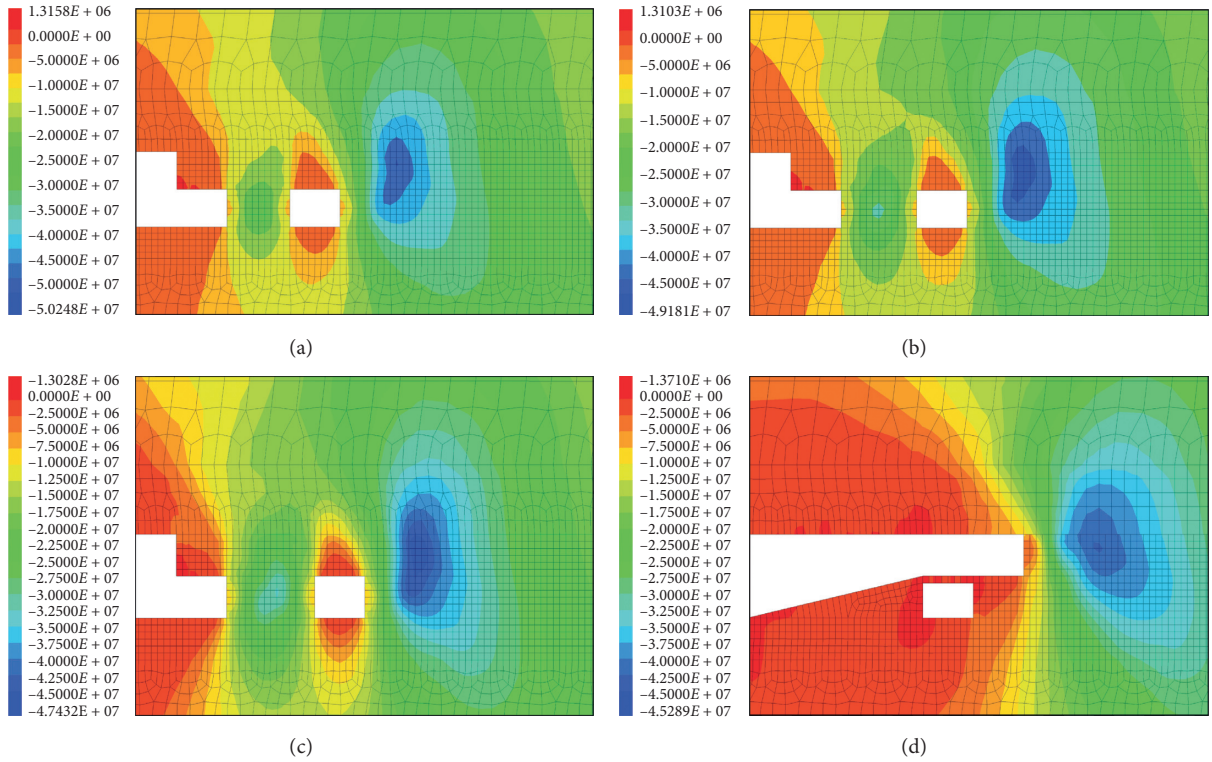

Figure 8: Vertical stress of gob-side entry. (a) 5 m. (b) 6 m. (c) 7 m. (d) −8 m.

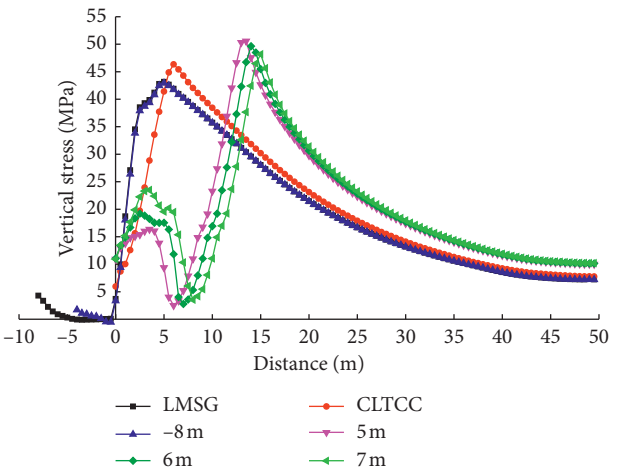

Figure 9: Vertical stress of solid coal.

According to the energy criterion, the risk of rock burst on the solid coal side is analyzed. Rock burst is a dynamic phenomenon caused by the destroying of the mechanical equilibrium state of the coal and rock masses system when the energy released is greater than the energy consumed. It can be expressed as [29]

$$\frac{dU_S}{dt} + \frac{dU_C}{dt} > \frac{dU_B}{dt}, \tag{15}$$

where U_S is energy stored in coal and rock masses; U_C is dynamic load energy; U_B is the energy consumed by rock burst.

The energy stored in the coal and rock masses is given:

$$U = \frac{\sigma^2}{2E}, \tag{16}$$

where σ is coal and rock load and E is elastic modulus.

Therefore, the energy stored in the coal body can be expressed as stress; that is, when the rock burst occurs, the conditions must be met [29]:

$$\sigma_1 + \sigma_2 > \sigma_{\min}, \tag{17}$$

where σ_1 is static load in coal and rock masses; σ_2 is dynamic load caused by mine earthquake; $\sigma_{\min}$ is the minimum load required for rock burst.

From the foregoing analysis, the peak value of vertical stress in the narrow coal pillar gob-side entry solid coal is relatively larger, and that in the NCPG is relatively smaller. So, under the same dynamic load conditions, the elastic energy stored in the NCPG coal and rock masses is less.

It is known from equation (15) that another key factor affecting the occurrence of rock burst is the size of U_B. That is to say, the energy consumption capability of coal and rock bodies needs to be analyzed. The destruction process of coal pillars is dynamic destruction, which is manifested by the instantaneous collapse and breakage of coal and rock masses, which will obtain more kinetic energy and are thrown into the roadway at a higher speed. Therefore, the energy U_B consumed by rock burst can be divided into the energy U_p consumed by coal and rock destruction and the kinetic

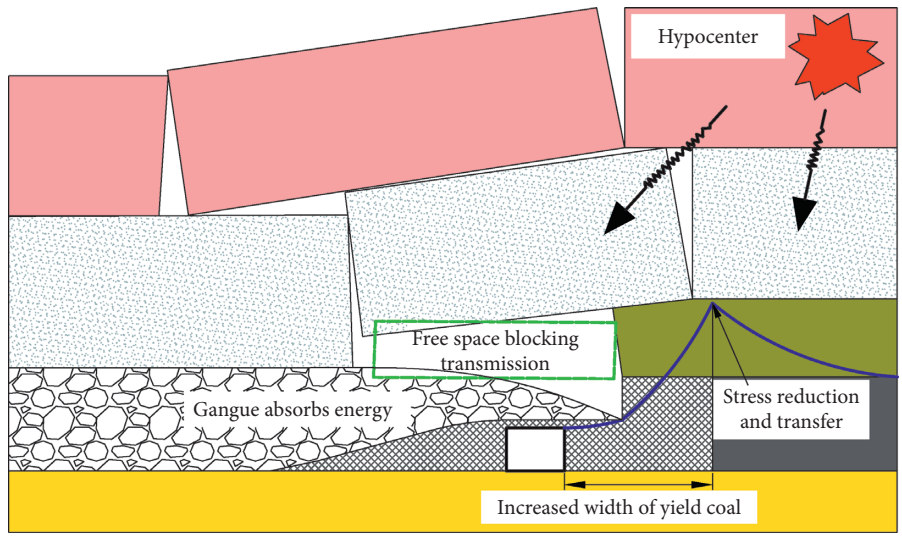

Figure 10: Principle of preventing rockburst.

energy U_k consumed by coal throwing. The relational expression is

$$U_B = U_p + U_k. \tag{18}$$

When rock burst occurs, it is mainly manifested as the energy consumed by the destruction of the plastic coal in the limit equilibrium zone. The relational expression is as follows:

$$U_p = \int_0^L \frac{\partial U_p}{\partial l} dl, \tag{19}$$

where L is the width of the limit equilibrium zone.

Equation (19) shows that when the rock burst occurs, the larger the width of the limit equilibrium zone is, the more energy is consumed for the plastic coal crushing. NCPG increases the width of the limit equilibrium zone by changing the position of the gob-side entry, so the energy consumed by plastic coal destruction is more than that of the narrow coal pillar gob-side entry.

The kinetic energy is consumed when the coal body is thrown out during the process of rock burst. If the critical initial velocity of the crushed coal and rock masses is du/dt, the kinetic energy of the crushed unit coal and rock masses is expressed as

$$U_{k'} = \frac{1}{2}\rho\left(\frac{du}{dt}\right)^2, \tag{20}$$

where ρ is coal density.

Researches have shown that the critical initial velocity of the crushed coal and rock masses with rock burst is 10 m/s. If ρ is 1.4×10^3 kg/m^3, the minimum kinetic energy of rock burst is 7×10^4 J/m^3 [29]. It is generally believed that when the kinetic energy released by the coal body is less than this value, the dynamic phenomenon of rock burst will not occur. The kinetic energy required for the coal body to be thrown out within the limit equilibrium zone is

$$U_k = \int_0^L \frac{1}{2}\rho\left(\frac{du}{dt}\right)^2 dl. \tag{21}$$

Equation (21) shows that the larger the range of the limit equilibrium zone is, the more kinetic energy is required to eject the coal body when rock burst occurs. Therefore, the kinetic energy consumed by the coal body of the limit equilibrium zone in the NCPG is more than that of the narrow coal pillar gob-side entry.

Based on the above analysis, a qualitative comparison of the energy in the two roadway arrangements can be obtained, as shown in Table 4. It can be found more intuitively that in NCPG coal and rock masses have lower energy storage and more energy consumption when the coal and rock energy is released. Therefore, NCPG is more advantageous than narrow coal pillar gob-side entry in preventing rock burst.

6. Advantages of NCPG to Prevent Rock Burst

NCPG has obvious advantages over conventional rock burst prevention technology, mainly reflected in the following aspects:

(1) Regional rock burst prevention of NCPG: conventional rockburst prevention technology mainly relies on monitoring points to predict the risk of rock burst and is usually implemented in areas affected by rock burst. However, there are certain errors in prediction results, and it is difficult to predict the risk of rock burst beyond the monitoring points. Due to the limitation of the risk prediction, it is difficult for conventional rock burst prevention technology to cover all areas of mining roadway. The NCPG is in the stress relief area as a whole, which can realize the prevention of regional rock burst in the mining roadway.

(2) Actively prevent rock burst: conventional rock burst prevention technology is implemented after the mining system or roadway is formed. At this time, the factors that induce rock burst already exist or start to function, lagging behind the rock burst risk.

Table 4: Qualitative comparison of energy.

Roadway layout	Stored energy (U_S)	Energy consumption (U_B)
Narrow coal pillar gob-side entry	More	Less
NCPG	Less	More

NCPG actively reduces the stress concentration of coal and rock masses by adjusting the roadway layout and eliminates the stress concentration environment of coal bodies around the roadway.

(3) NCPG has security: conventional rock burst prevention technology measures are implemented in impact hazardous areas. During the implementation process, rock burst may occur, which has a relatively high risk. The NCPG is far away from the stress concentration area, and the safety is improved during the excavation and mining.

(4) Timeliness of prevention: the effect of conventional rock burst prevention technology to prevent rock burst cannot be guaranteed for a long time. For example, coal seam water inject measures can achieve the prevention of rock burst by reducing the impact properties of coal, but the risk of rock burst will be restored due to the stop of water injection. The prevention effect of the destress boreholes will be weakened or will disappear over time.

(5) Achieve efficient production: conventional technology measures require that production should be stopped during implementation, and parallel operations cannot be achieved. There is a contradiction between the implementation of rock burst prevention technology and production. But NCPG does not affect the mining of the panel after the excavation of the roadway is completed and can achieve efficient production of the panel.

Dialectically looking at problems is conducive to the development of things. The analysis proves that NCPG has significant advantages in the prevention of rock burst, but it still has several drawbacks. Its application conditions are subject to certain restrictions, which is mainly suitable for thick coal mining. Besides, we must pay attention to the problem of air leakage along the gob-side entry to the goaf.

7. Practical Experiences of NCPG

7.1. Geological Conditions. Huafeng coal mine is a typical rock burst mine in China, and there have been many rock burst accidents in history. At present, the mining depth has reached 1300 m and the confining pressure of the original rock stress field is high, which belongs to the high-stress mine. CLTCC was adopted for the underground mining of 4# coal seam, whose average thickness is 6.2 m. The 4# coal seam has a strong rock burst tendency, and the immediate roof has a moderate rock burst tendency. Based on the idea of avoiding high-pressure concentration areas to prevent rock burst, narrow coal pillar gob-side entry technology was adopted, but rock burst accidents still occurred in 1411 tail gate. Figure 11 shows two photographs of the roadway's large deformation and rock burst accident when gob-side entry driving technology with 5 m coal pillars is used. In the gob-side entry, large deformation occurred on the side of the coal pillar, and rock burst mainly occurred on the solid coal side. This led to an immediate shutting down of this panel for several months and an overall economic loss of several millions of dollars.

7.2. Application Effect of NCPG. Based on the study of the abutment pressure distribution around the gob-side entry, the negative coal pillar roadway layout technology was applied to 1411 tail gate. The roadway layout relationship is given in Figure 12.

The head gate of 1410 panel was driven along the coal seam roof, and its limit equilibrium zone width is 15.8 m. Based on the discussion about coal pillar width, the tail gate of 1411 panel adopts a negative coal pillar (–10 m) roadway layout, and the distance between the roadway and the peak position of abutment pressure increased to 21.9 m. This made it feasible to arrange the 1411 tail gate in the low-stress area of high-stress mine. During the service of the NCPG, the roof pressure of the hydraulic prop was monitored using a circular chart pressure autometer, and the deformation of the surrounding rock was observed using the cross observation method. Roof pressure of the gob-side entry indicates the gob pressure above the entry since the entry is located under the gob edge. The obtained data are plotted in Figure 13. The data shows that roof pressure is bout 1.4 MPa, which is maintained at a low level without many fluctuations. The comparison demonstrates that the numerical modeling is consistent with the stress distribution monitored on site. Besides, it does not show the rule of the roof pressure of the conventional roadway, which increases first and then decreases with the distance ahead of the working face. This proves that the gob-side entry is independent of the side and front abutment pressures. The gob-side entry mainly bears the pressure of the gangue collapse in the goaf, which is attributed to the protective function of the key block. The amount of gob-side entry deformation is also significantly low. The approaching distance of the roof and floor is about 29 mm, generally less than 25 mm, and the convergence of the two sides is about 23 mm. The support effect during the roadway service is shown in Figure 14. Through the application of NCPG in 1411 tail gate, no more rock burst disasters have occurred, which effectively prevented the rock burst disaster.

In production practice, the 1410 panel has the advancing speed of 1 m/d due to the implementation of the technology to prevent rock burst. After adopting NCPG, the advancing speed of the panel was increased to 2.4 m/d. The production efficiency has been doubled and the economic benefits brought by it have accumulated to $160 million. Besides, per meter of roadway of

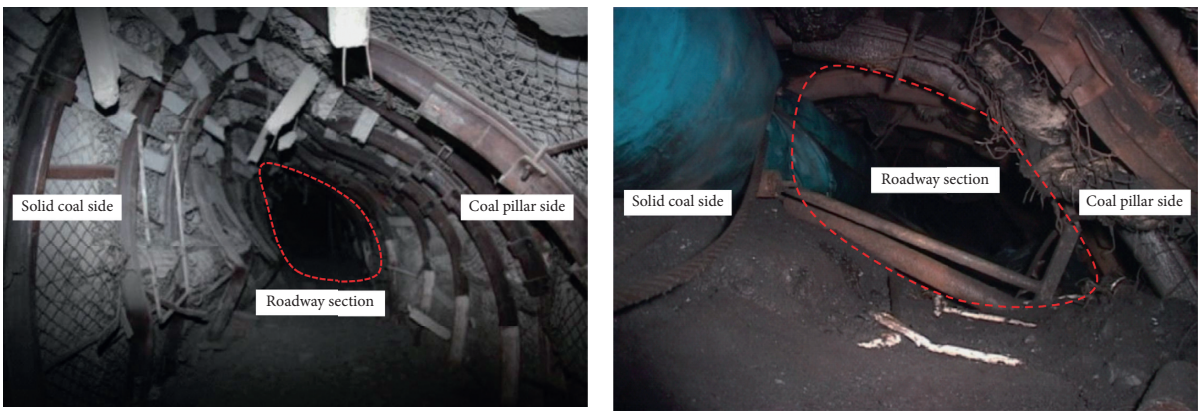

(a) (b)

Figure 11: Photos of large deformation and rock burst in 1411 tail gate. (a) Roadway large deformation. (b) Roadway rock burst.

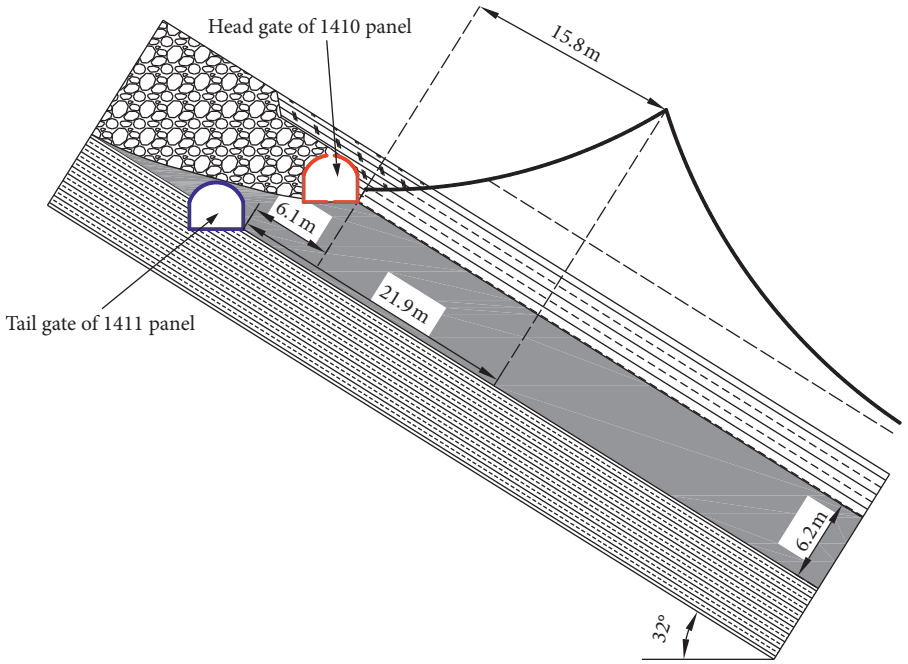

Figure 12: Schematic diagrams of roadway position relationship.

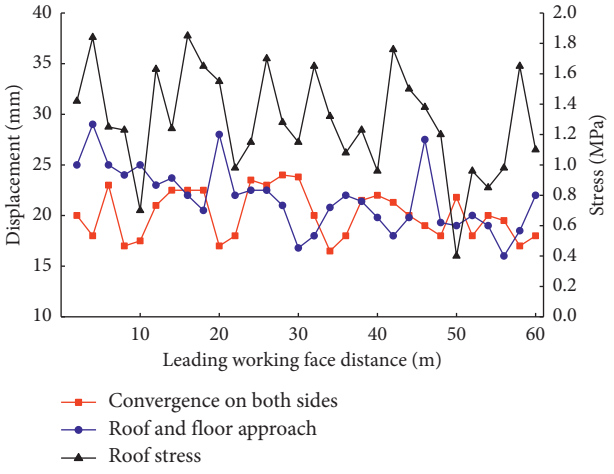

Figure 13: Displacement and roof pressure of the tail gate of panel 1411.

Figure 14: Service effect of the 1411 tail gate.

NCPG can reduce the coal pillar loss by 124 m^3 and the coal loss at the panel end by 67.2 m^3, a total of 191.2 m^3, and economic benefits of US $60 million can be obtained.

8. Conclusion

In this paper, NCPG is proposed to prevent rock burst. The stress distributions of the surrounding rock of narrow coal pillar gob-side entry and NCPG are compared and analyzed. We can obtain several conclusions as follows:

(1) The physical modeling results demonstrate that the trapezoidal coal body is in a low-stress zone which is much lower than the rock stress, and the peak value of vertical stress in solid coal is lower than that of the conventional panel. The calculation of the mechanical model shows that the width of the limit equilibrium zone of the solid coal in LMSG is reduced by a small proportion compared with the conventional working face.

(2) The stress at both ends of the NCPG is lower than that of the narrow coal pillar gob-side entry. NCPG is always in a low-stress area after excavation, and its peak stress of solid coal does not change, but the width of the limit equilibrium zone increases, so the degree of stress concentration decreases. NCPG achieves the effect of transferring concentrated stress to deep coal body and plays the role of pressure avoidance.

(3) Based on the energy criterion, the energy stored in the NCPG coal and rock masses is lower than that of narrow coal pillar gob-side entry, and more energy will be consumed when it is released. Therefore, the NCPG is more conducive to preventing rock burst. NCPG has significantly improved the regionality, initiative, safety, and timeliness of rock burst prevention in deep high-stress coal seam mining. Huafeng coal mine 1411 tail gate applied NCPG layout technology, and no rock burst occurred during the service period.

Data Availability

The data used to support the findings of this study are available from the corresponding author upon request.

Conflicts of Interest

The authors declare no conflicts of interest.

Acknowledgments

This work was supported by the National Natural Science Foundation of Surface Project of China (nos. 51774289 and 52074291), the National Natural Science Foundation of the Youth Science Foundation of China (no. 51404270), and the Open Fund of State Key Laboratory of Green and Safe Development of Western Coal (SKLCRKF1903).

References

[1] B.-R. Chen, X.-T. Feng, Q.-P. Li, R.-Z. Luo, and S. Li, "Rock burst intensity classification based on the radiated energy with damage intensity at Jinping ii hydropower station, China," *Rock Mechanics and Rock Engineering*, vol. 48, no. 1, pp. 289–303, 2015.

[2] M. C. He, F. Zhao, M. Cai, and S. Du, "A novel experimental technique to simulate pillar burst in laboratory," *Rock Mechanics and Rock Engineering*, vol. 48, no. 5, pp. 1833–1848, 2015.

[3] C.-P. Lu, G.-J. Liu, Y. Liu, N. Zhang, J.-H. Xue, and L. Zhang, "Microseismic multi-parameter characteristics of rockburst hazard induced by hard roof fall and high stress concentration," *International Journal of Rock Mechanics and Mining Sciences*, vol. 76, pp. 18–32, 2015.

[4] G. Brauner, *Rockbursts in Coal Mines and Their Prevention*, Routledge, Milton Park, AB, USA, 2017.

[5] S. Zhu, Y. Feng, F. Jiang, and J. Liu, "Mechanism and risk assessment of overall-instability-induced rockbursts in deep island longwall panels," *International Journal of Rock Mechanics and Mining Sciences*, vol. 106, pp. 342–349, 2018.

[6] Z.-l. Li, X.-Q. He, L.-M. Dou, D.-Z. Song, and G.-F. Wang, "Numerical investigation of load shedding and rockburst reduction effects of top-coal caving mining in thick coal seams," *International Journal of Rock Mechanics and Mining Sciences*, vol. 110, pp. 266–278, 2018.

[7] J. He, L. Dou, S. Gong, J. Li, and Z. Ma, "Rock burst assessment and prediction by dynamic and static stress analysis based on micro-seismic monitoring," *International Journal of Rock Mechanics and Mining Sciences*, vol. 93, pp. 46–53, 2017.

[8] E. T. Brown, "Rockburts: prediction and control," *Tunneling Journal*, vol. 16, no. 4, pp. 17–19, 1984.

[9] X. S. Liu, Y. L. Tan, J. G. Ning, Y. W. Lu, and Q. H. Gu, "Mechanical properties and damage constitutive model of coal in coal-rock combined body," *International Journal of Rock Mechanics and Mining Sciences*, vol. 110, pp. 140–150, 2018.

[10] W. D. Ortlepp and T. R. Stacey, "Rockburst mechanisms in tunnels and shafts," *Tunnelling and Underground Space Technology*, vol. 9, no. 1, pp. 59–65, 1994.

[11] T. H. Ma, C. A. Tang, L. X. Tang, W. D. Zhang, and L. Wang, "Rockburst characteristics and microseismic monitoring of deep-buried tunnels for Jinping II Hydropower Station," *Tunnelling and Underground Space Technology*, vol. 49, pp. 345–368, 2015.

[12] A. C. Adoko, C. Gokceoglu, L. Wu, and Q. J. Zuo, "Knowledge-based and data-driven fuzzy modeling for rockburst prediction," *International Journal of Rock Mechanics and Mining Sciences*, vol. 61, pp. 86–95, 2013.

[13] S. L. Song, X. S. Liu, Y. L. Tan, D. Y. Fan, Q. Ma, and H. L. Wang, "Study on failure modes and energy evolution of

coal-rock combination under cyclic loading," *Shock and Vibration*, vol. 2020, Article ID 5731721, 16 pages, 2020.

[14] P. Wang, H. Jia, and P. Zheng, "Sensitivity Analysis of Bursting liability for different coal-rock combinations based on their inhomogeneous characteristics," *Geomatics, Natural Hazards and Risk*, vol. 11, no. 1, pp. 149–159, 2020.

[15] A. Z. Toper, K. K. Kabongo, R. D. Stewart, and A. Daehnke, "The mechanism, optimization and effects of preconditioning," *Journal of the Southern African Institute of Mining and Metallurgy*, vol. 100, no. 1, pp. 7–15, 2000.

[16] D. Fan, X. Liu, Y. Tan et al., "Roof cutting parameters design for gob-side entry in deep coal mine: a case study," *Energies*, vol. 12, no. 10, pp. 2032–2057, 2019.

[17] Z.-L. Li, L.-M. Dou, W. Cai, G.-F. Wang, Y.-L. Ding, and Y. Kong, "Roadway stagger layout for effective control of gob-side rock bursts in the longwall mining of a thick coal seam," *Rock Mechanics and Rock Engineering*, vol. 49, no. 2, pp. 621–629, 2016.

[18] Q. Zhu, Y. Feng, M. Cai, J. Liu, and H. Wang, "Interpretation of the extent of hydraulic fracturing for rockburst prevention using microseismic monitoring data," *Journal of Natural Gas Science and Engineering*, vol. 38, pp. 107–119, 2017.

[19] Z. Zheng, Y. Xu, D. Li, and J. Dong, "Numerical analysis and experimental study of hard roofs in fully mechanized mining faces under sleeve fracturing," *Minerals*, vol. 5, no. 4, pp. 758–777, 2015.

[20] Q. X. Qi, Y. Z. Li, S. K. Zhao et al., "Seventy years development of coal mine rockburst in China: establishment and consideration of theory and technology system," *Coal Science and Technology*, vol. 47, no. 9, pp. 1–40, 2019, in Chinese.

[21] L. Jiang, P. Zhang, L. Chen et al., "Numerical approach for goaf-side entry layout and yield pillar design in fractured ground conditions," *Rock Mechanics and Rock Engineering*, vol. 50, no. 11, pp. 3049–3071, 2017.

[22] L.-M. Dou, Z.-L. Mu, Z.-L. Li, A.-Y. Cao, and S.-Y. Gong, "Research progress of monitoring, forecasting, and prevention of rockburst in underground coal mining in China," *International Journal of Coal Science and Technology*, vol. 1, no. 3, pp. 278–288, 2014.

[23] J. L. Zhao and J. Wu, "Whole seam longwall mining with split-level gateways (LMSG) in thick coal seams," 2002.

[24] Z. Q. Wang, L. Shi, P. Wang, and C. Wu, "Influence of lateral structure and combined support system of split-level entries in the thick seam," *Arabian Journal of Geosciences*, vol. 13, p. 1043, 2020.

[25] M. G. Qian, P. W. Shi, and J. L. Xu, *Ground Pressure and Strata Control*, China University of Mining and Technology Press, Xuzhou, China, 2010, in Chinese.

[26] L. S. Jiang, P. Wang, P. Q. Zheng, H. J. Luan, and C. Zhang, "Influence of different advancing directions on mining effect caused by a fault," *Advances in Civil Engineering*, vol. 2019, Article ID 7306850, 10 pages, 2019.

[27] Z. Q. Wang, *Research on strata pressure laws working face lapped each other of the stagger arrangement roadway layouts in thick coal seams*, Ph.D. thesis, China University of Mining and Technology, Beijing, China, 2011, in Chinese.

[28] G. Feng, P. Wang, and Y. P. Chugh, "A new gob-side entry layout for longwall top coal caving," *Energies*, vol. 11, no. 5, pp. 1292–1316, 2018.

[29] L. M. Dou, Z. L. Mou, A. Y. Cao, S. Y. Gong, H. He, and C. P. Lu, *Prevention and Control of Colliery Impact on Mining Industry*, Beijing Science Press, Beijing, China, 2019, in Chinese.